19980423 117

Reexamination of Fault Angles Predicted by Shear Localization Theory

J. W. Rudnicki[1] and W. A. Olsson[2]

[1]Department of Civil Engineering, Northwestern University Evanston, IL 60208-3109 USA

[2]Geomechanics Department, Sandia National Laboratories, Albuquerque, NM 87185-0751 USA

ABSTRACT

This paper reexamines orientations of shear bands (fault angles) predicted by a theory of shear localization as a bifurcation from homogeneous deformation. In contrast to the Coulomb prediction, which does not depend on deviatoric stress state, the angle between the band normal and the least (most compressive) principal stress increases as the deviatoric stress state varies from axisymmetric compression to axisymmetric extension. This variation is consistent with the data of Mogi (1967) on Dunham dolomite for axisymmetric compression, extension and biaxial compression, but the predicted angles are generally less than observed. This discrepancy may be due to anisotropy that develops due to crack growth in preferred orientations. Results from specialized constitutive relations for axisymmetric compression and plane strain that include this anisotropy indicate that it tends to increase the predicted angles. Measurements for a weak, porous sandstone (Castlegate) indicate that the band angle decreases with increasing inelastic compaction that accompanies increasing mean stress. This trend is consistent with the predictions of the theory but, for this rock, the observed angles are less than predicted.

KEYWORDS

INTRODUCTION

One of the most easily observable features of rock deformation tests is the angle that the failure plane (fault surface) makes with the direction of the applied loading. This angle, when measured between the normal to the plane and the direction of the most compressive principal stress is nearly always greater than 45°. This inclination is typically explained in terms of the Coulomb condition (Jaeger and Cook, 1969) and given as

$$\theta_c = 45^0 + \frac{1}{2}\arctan\mu_c \qquad (1)$$

where μ_c is the Coulomb friction coefficient, often written as the tangent of the friction angle ϕ. For typical values of μ_c, 0.6 to 0.75, values of θ_c range from 60.5° to 81.9°, which is comparable to the range of observed failure plane angles. Closer examination suggests, however, that the expression Eqn. (1) is an inadequate,

DISCLAIMER

or at least incomplete, prediction. The Coulomb prediction does not depend at all on the stress state. In contrast, experiments on rocks (Mogi, 1967; Handin et al., 1967) do reveal that the failure angle is different for axisymmetric compression and axisymmetric extension, indicating a dependence on the deviatoric stress state. Furthermore, the dependence of the Coulomb angle on material properties is limited. As emphasized by Handin (1969), "In a cohesive material, however, internal friction is a fictitious quantity that cannot be measured directly....[it] should be regarded as no more than the slope of the Mohr envelope for intact rock."

This paper reexamines the predictions of an approach to failure (Rudnicki and Rice, 1975) as bifurcation, or non-uniqueness, from homogeneous deformation. In particular, conditions are sought for which the material behavior allows a solution alternative to homogeneous deformation and corresponding to concentrated shear deformation in a planar band. The prediction for the orientation of the band has been given by Rudnicki and Rice (1975) but is rewritten here in a form that is comparable to that for the Coulomb prediction. In addition we compare the predictions with those of other analyses for the specific deformation states of axisymmetric compression and plane strain. These analyses are based on the approach of Rudnicki and Rice (1975) but use constitutive relations that include anisotropy.

The predictions are compared with experimental results of Mogi (1967) and Handin et al.(1967) for the dependence of the band angle on the deviatoric stress state. Comparison of the predictions with new measurements on Castlegate sandstone indicate that the band angle decreases with a change from dilating to compacting behavior that accompanies increasing compressive mean stress.

ANALYSIS OF LOCALIZATION

Band formation is subject to conditions of kinematic compatibility and continuing equilibrium. The kinematic condition arises from the requirement that the velocity field remain continuous at the inception of band formation (though the velocity may become discontinuous as localization proceeds). This restricts the difference in the strain-rates inside and outside the band to have the form:

$$\dot{\varepsilon}^b_{ij} = \dot{\varepsilon}^0_{ij} + \frac{1}{2}(n_i g_j + n_j g_i)$$ (2)

where the n_i are components of the unit normal to the band and the g_i are functions of distance across the band. Thus, the difference field is a combination of shear and compression relative to the band and the intermediate principal value of the difference field is zero. Since this is similar to a plane strain type of deformation, plane strain states tend to be more favorable for localization than axisymmetric ones. If the material is to remain in equilibrium at the inception of band formation, then traction rates across the band boundary must be equal:

$$n_i \dot{\sigma}^b_{ij} = n_i \dot{\sigma}^0_{ij}$$ (3)

When these requirements are combined with constitutive relations of the form

$$\dot{\sigma}_{ij} = L_{ijkl}\dot{\varepsilon}_{kl}$$ (4)

the result is

$$(n_i L_{ijkl} n_l)g_k = n_i(L - L^0)_{ijkl}\dot{\varepsilon}^0_{kl}$$ (5)

In the simplest case, the material inside and outside the band is assumed to be the same at the instant of band formation, $L = L^0$, and the problem reduces to a nonlinear eigenvalue problem for the g_k:

$$(n_i L_{ijkl} n_l)g_k = 0$$ (6)

(Rice and Rudnicki (1980) have shown that band formation based on the assumption of continued inelastic loading outside the band at the instant of formation precedes that allowing for elastic unloading outside the band.) Band formation corresponds to a non-trivial solution for the g_i and is possible when

$$\det(n_i L_{ijkl} n_l) = 0$$ (7)

The predictions discussed here correspond to finding the orientation (value of n_i) and values of the constitutive parameters at which this condition is first met.
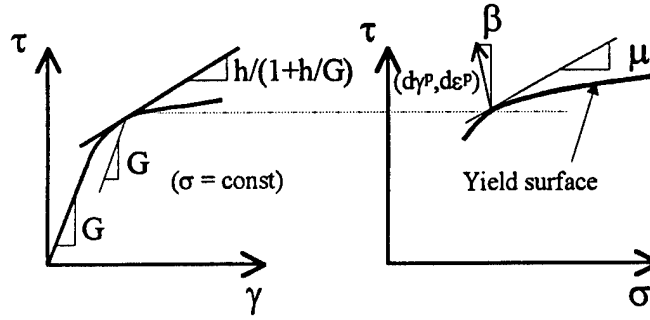
Figure 1. Geometric interpretation of constitutive parameters.

CONSTITUTIVE RELATION

A constitutive relation describing some features of brittle rock deformation has the following form for the simple stress state combining pure shear τ and hydrostatic compression σ:

$$d\gamma = \frac{d\tau}{G} + \frac{1}{h}(d\tau - \mu d\sigma) \tag{8}$$

$$d\varepsilon = -\frac{d\sigma}{K} + \frac{\beta}{h}(d\tau - \mu d\sigma) \tag{9}$$

where $d\gamma$ and $d\varepsilon$ are increments of shear strain and volume strain. The first terms are elastic contributions; the second terms are inelastic. Inelastic shear strain is inhibited by hydrostatic compression and μ is a friction coefficient. The ratio of increments of inelastic volume strain to inelastic increments of shear strain is β. Thus, β is a dilation coefficient, positive for dilation, negative for compaction. The geometric meaning of these parameters is shown in Figure 1: h is related to the slope of the τ vs. γ curve at constant mean stress (σ) as shown; μ is the local slope of the yield surface in stress space, dividing regions of elastic unloading from regions of further inelastic response. Note that the inelastic strain increment is normal to this yield surface if $\mu = \beta$.

PREDICTIONS OF BAND ORIENTATION

When Eqn. (8) and Eqn. (9) are generalized to arbitrary stress states, as in Rudnicki and Rice (1975), the prediction for the angle between the band normal and the least (most compressive) principal stress is

$$\theta = \frac{\pi}{4} + \frac{1}{2}\arcsin\alpha \tag{10}$$

where

$$\alpha = \frac{(2/3)(1+\nu)(\beta+\mu) - N(1-2\nu)}{\sqrt{4-3N^2}} \tag{11}$$

and

$$N = \sigma'_{II}/\bar{\tau} \tag{12}$$

describes the deviatoric stress state; σ'_{II} is the intermediate principal deviatoric stress and $\bar{\tau} = \sqrt{\frac{1}{2}\sigma'_{ij}\sigma'_{ij}}$ is the Mises equivalent stress. N ranges from $-1/\sqrt{3}$ for axisymmetric extension to $1/\sqrt{3}$ for axisymmetric compression. Thus, the deviation of the band angle from the maximum shear direction (45°) is proportional to the mean of β and μ and depends on the deviatoric stress state described by N. Eqn. (11) is valid for $-1 \leq \alpha \leq 1$. A conservative bound on the sum of the dilatancy factor and friction coefficient that ensures α meets this condition is $-\sqrt{3} \leq (\beta+\mu) \leq \sqrt{3}$ (not $\sqrt{3}/2$, as reported by Rudnicki and Rice. This correction has been pointed out and discussed by Perrin and Leblond (1993)). If α exceeds 1, then $\theta = 90°$ and if α is less than -1, $\theta = 0°$. Note that for an inelastically compacting material $\beta < 0$, and if the magnitude of β exceeds μ, the band angle can be less than 45°.
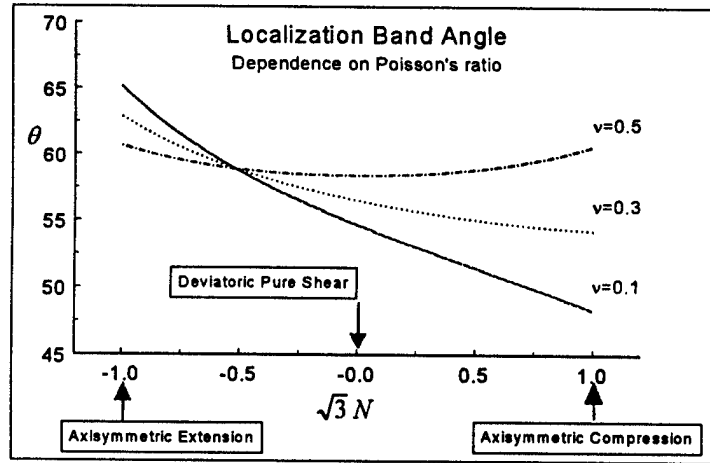
Figure 2.

If the material is elastically incompressible, $\nu = 1/2$ (probably not realistic for rock), Eqn. (11) reduces to the simpler expression

$$\alpha = \frac{(\beta + \mu)}{\sqrt{4 - 3(\sigma'_{II}/\bar{\tau})^2}} \tag{13}$$

For an incompressible material and axisymmetric stress states ($N = \pm 1/\sqrt{3}$)

$$\alpha = (\beta + \mu)/\sqrt{3} \tag{14}$$

For an incompressible material and deviatoric pure shear ($N = 0$)

$$\alpha = (\beta + \mu)/2 \tag{15}$$

During a plane strain test, the value of N evolves. The elastic value for plane strain is

$$N = \pm(1 - 2\nu)/\sqrt{3(1 - \nu + \nu^2)}$$

with the positive sign pertaining for compression and the negative for tension. As ν varies from 0 to 0.5, N decreases from the value for axisymmetric compression ($N = 1/\sqrt{3}$) to that for deviatoric pure shear ($N = 0$). For $\nu = 0.2$ and 0.3, $N = 0.378$ and 0.260. As inelastic strains become larger than elastic strains, N approaches $-2\beta/3$ and the intermediate principal value of the deviatoric *plastic* strain-rate approaches zero. In this limit, the expression for α can be rewritten as

$$\alpha = \frac{\beta(2 - \nu) + (1 + \nu)\mu}{\sqrt{9 - \beta^2}}$$

Figures 2-4 plot the predicted band angle against $\sqrt{3}N$ for various combinations of parameters. Figure 2 shows the results for $\beta + \mu = 0.9$ and three values of Poisson's ratio ν : 0.1, 0.3 and 0.5. Figure 3 shows results for $\nu = 0.2$ and five values for the sum $\beta + \mu$, 0.0, 0.3, 0.6, 0.9 and 1.2. Figure 4 compares the results for $\beta + \mu = 0.9$ and $\nu = 0.2, 0.5$ with predictions of the Coulomb angle. Note that the Coulomb prediction depends only on the friction coefficient and not at all on the stress state. Although the ranges of numerical values of μ and μ_c are similar, in general, there is no direct relation between them. If, however, the stress state is assumed to be axisymmetric and to satisfy simultaneously the yield condition and the Coulomb condition, the two friction coefficients are related by

$$\sin \phi = \frac{3\mu}{2\sqrt{3} \pm \mu} \tag{16}$$

where $\mu_c = \tan \phi$ and the (+) sign is for compression and the (−) sign for extension. If $\mu = 0.6$, the corresponding values of μ_c for compression and extension are 0.474 and 0.727.

Localization Band Angle
Dependence on β+μ

1.2
0.9
0.6
0.3
0.0

θ

Deviatoric Pure Shear

$\sqrt{3}\,N$

Axisymmetric Extension

Axisymmetric Compression

Figure 3.

Localization Band Angle
Comparison with Coulomb Angle

μ_c=0.727
μ_c=0.6
μ_c=0.474

θ

$\nu = 0.5$

$\nu = 0.2$

Deviatoric Pure Shear

$\sqrt{3}\,N$

Axisymmetric Extension

Axisymmetric Compression
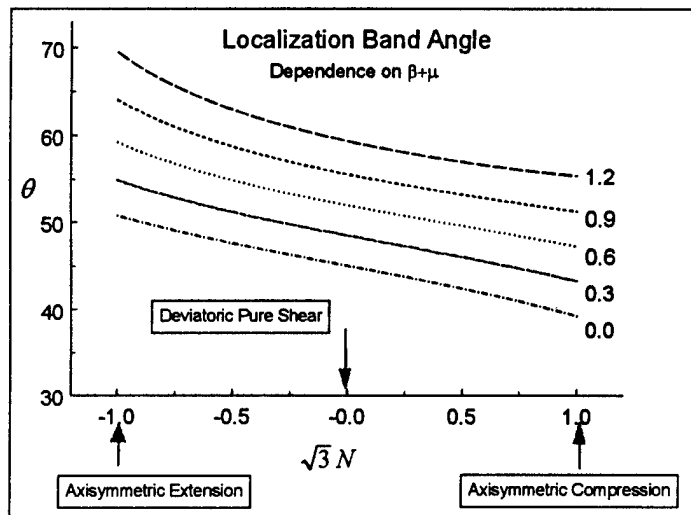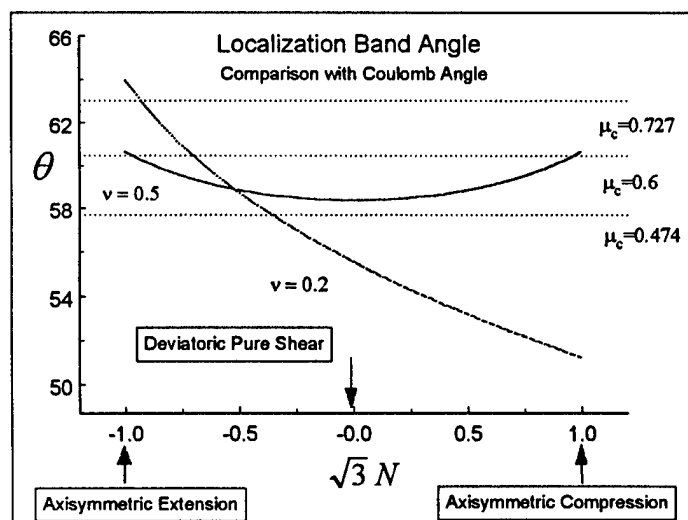
Figure 4.

PREDICTIONS FOR SPECIAL DEFORMATION STATES

The constitutive relation upon which the prediction Eqn. (10), with Eqn. (11), is based is valid for arbitrary deformation states, but it assumes isotropic elasticity and isotropic hardening of the yield surface. In this section, the results are compared with predictions based on constitutive relations that include anisotropy but are limited to special deformation states.

Axisymmetric Compression

Rudnicki (1977) has analyzed localization in axisymmetric compression for a constitutive relation intended to include the anisotropy that develops due to preferential microcrack growth in the axial direction. Although the parameters are expressed in a form that differs from that of Rudnicki and Rice (1975), the principal difference in the constitutive relation used by Rudnicki (1977) is the appearance of two shear moduli. The modulus G_l governs increments of shearing in the longitudinal direction (parallel to the axis of symmetry); G_t governs shearing transverse to the symmetry axis. The prediction for the band angle can be expressed in the form of Eqn. (10) but with α given by

$$\alpha = \frac{\sqrt{(r + \hat{G}_l)(2\nu + \hat{G}_l)} - (1 + \hat{G}_l + \hat{G}_t)}{\sqrt{(r + \hat{G}_l)(2\nu + \hat{G}_l)} + (1 - \hat{G}_l + \hat{G}_t)} \tag{17}$$

where $\hat{G}_l = G_l/(9K/4)$, $\hat{G}_t = G_t/(9K/4)$, K is an in-plane, incremental bulk modulus (not necessarily elastic), r is a parameter expressing the pressure dependence, and ν is not Poisson's ratio but another incremental parameter expressing the dilation. Rudnicki (1977) has given a more detailed discussion of the meaning of these parameters and their relation to the parameters used by Rudnicki and Rice (1975).

Because the parameters of this relation do not correspond directly to those of Rudnicki and Rice (1975), it is worthwhile to consider a number of special cases. If both $\hat{G}_l$ and $\hat{G}_t$ are much less than unity, then Eqn. (17) reduces to

$$\alpha = \frac{\sqrt{2r\nu} - 1}{\sqrt{2r\nu} + 1} \tag{18}$$

Note that in order for band angles to be greater than $45°$, $2r\nu > 1$. If the material is completely incompressible then $\nu = 0.5$ and Eqn. (18) reduces further to

$$\alpha = \frac{\sqrt{r} - 1}{\sqrt{r} + 1} \tag{19}$$

In this case, $\alpha = \mu/\sqrt{3}$ for the constitutive relation used by Rudnicki and Rice (1975) and, consequently, it is possible to derive the relation

$$r = \left(\frac{\sqrt{3} + \mu}{\sqrt{3} - \mu}\right)^2$$

For example, if $\mu = 0.6$, $r = 4.25$ and for $\mu = 0.75$, $r = 6.39$. If normality is satisfied (flow rule is associated), $r = 2\nu$ and Eqn. (17) reduces to

$$\alpha = \frac{r - (1 + \hat{G}_t)}{r + (1 + \hat{G}_t)} \tag{20}$$

In order to examine the effects of differences between G_l and G_t, first choose r, ν, and $\hat{G}_t = \hat{G}_l$ so that the predicted band angle is same as for values of the constitutive parameters of the Rudnicki and Rice (1975) relation. If $r = 6.5$, $\nu = 0.77$, and $\hat{G}_t = \hat{G}_l = 1.19$, the band angle predicted from Eqn. (17) is $51.2°$, the same as that predicted from Eqn. (11) with $\beta = 0.3$, $\mu = 0.6$, and $\nu = 0.2$. If $\hat{G}_t$ is reduced to 75%, 50%, and 25% of $\hat{G}_l$, then the band angles increase to $53.2°$, $55.6°$, and $58.3°$, respectively. If $\hat{G}_t = 0$, then the band angle is $61.5°$.

Chau and Rudnicki (1990) have studied bifurcations, including localization in plane strain. Their analysis extends to compressible materials previous studies by Hill and Hutchinson (1975), Young (1976), and Needleman (1979). Again the prediction for the band angle can be written in the form of Eqn. (10) but α is given by

$$\alpha_{pl} = \frac{\sqrt{1+\delta+(1+\alpha)/\kappa} - \sqrt{1-\delta+(1-\alpha)/\kappa}}{\sqrt{1+\delta+(1+\alpha)/\kappa} + \sqrt{1-\delta+(1-\alpha)/\kappa}} \tag{21}$$

If the material is incompressible, $\kappa \to \infty$ and, in this case, α_{pl} is equal to the value given by Eqn. (11) (with $\beta = 0$ and $\nu = 0.5$) if

$$\delta = \frac{\mu}{1+\mu^2/4} \tag{22}$$

EXPERIMENTAL OBSERVATIONS

Most of the existing data on shear band orientations in rocks is for low porosity rock types such as granite and limestone. Because of their importance in oil and gas reservoirs, weak, porous rocks are of interest. A suite of samples from an axisymmetric testing program (unpublished data from D. H. Zeuch) of the weak Castlegate sandstone with a porosity of about 25% was available for examination. The specimens were right circular cylinders 50 mm in diameter by 100 mm in length. They were deformed in axisymmetric compression at 5 different confining pressures from 3.45 to 69 MPa (Table 1). The specimens were air-dry and vented to the atmosphere. Axial deformation was measured with a pair of linear variable differential transducers (LVDT) from endcap to endcap. Specimen diameter was monitored with an additional LVDT mounted at the midheight. Axial strain rate was 3×10^{-5} /sec.

TABLE 1. SHEAR BAND ANGLES FOR CASTLEGATE SANDSTONE

Test ID	Conf. Press.	μ	ν	β	θ eqn. (10)	θ measured
CG10	3.45	0.87	0.50	1.13	90	60
CG11	3.45	0.87	0.50	1.28	90	61
CG3	6.9	0.87	0.37	0.83	72	50
CG6	6.9	0.87	0.37	0.76	70	60
CG12	6.9	0.87	0.44	1.08	90	61
CG2	17.2	0.87	0.36	0.80	71	60
CG7	17.2	0.87	0.43	0.83	76	55
CG13	17.2	0.87	0.33	0.72	67	57
CG4	34.5	0.30	0.29	0.79	57	54
CG8	34.5	0.30	0.48	0.85	65	44
CG14	34.5	0.30	0.35	0.74	58	46
CG5	69	0.30	0.23	-0.29	40	none
CG9	69	0.30	0.18	0.45	49	none
CG15	69	0.30	0.18	-0.39	38	none

Computation of theoretical shear band (fault) orientation, θ, requires knowledge of ν, β and μ. Because β and ν vary throughout the straining of a given specimen, numerous partial unload cycles were imposed during each test, which allowed the values of β and ν near the point of localization to be evaluated for input to Eqn. (10) and Eqn. (11). A plot of $\bar{\tau}$ against σ for peak stress gave an estimate of μ.

All specimens deformed at confining pressures below 69 MPa developed one or more shear bands; several showed conjugate relationships. Specimens deformed at 69 MPa barreled but did not develop shear bands. Using a machinist's protractor, the angles between the maximum compression direction and the shear bands were measured near the center of the specimen to within approximately ± 1 degree. In half the cases the angles
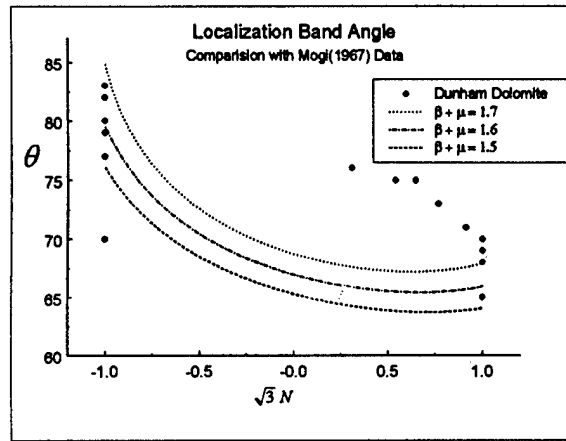
Figure 5.

were taken off the impression left on the inside of the polyolefin jackets.

DISCUSSION

Detailed comparison of the predictions with observations is difficult for several reasons. There have been few precise measurements of the values of the friction coefficient μ and the dilatancy factor β entering the predictions. As mentioned in the preceding section, these parameters (and possibly Poisson's ratio ν) generally evolve with inelastic shear strain and with mean stress. The values entering the predictions should be those just prior to localization An additional problem is the paucity of studies on the effects of the deviatoric stress state. Two of the very few studies of the dependence of the failure angle on deviatoric stress state (N) are those of Mogi (1967) and of Handin *et al.* (1967).

Mogi (1967) reported results of axisymmetric compression and extension tests on three rocks, Westerly granite, Dunham dolomite, and Solenhofen limestone. In addition, he performed biaxial compression tests on the dolomite. If the third principal stress is zero, as in these tests, the value of N depends as follows on s, the ratio of the lesser to greater applied compressive stress:

$$N = \frac{1}{\sqrt{3}} \frac{1 - 2s}{\sqrt{1 - s + s^2}}$$

(Mogi (1971) further investigated the effect of the intermediate principal stress on failure using a true triaxial apparatus, but, unfortunately, did not report failure angles.)

Figure 5 plots Mogi's (1967) results for the Dunham dolomite against the deviatoric stress state parameter $\sqrt{3}N$. Shown for comparison are the predictions of Eqn. (10) for $\nu = 0.3$ and three values of the sum $\beta + \mu$, 1.5, 1.6, and 1.7. The data, in agreement with the theoretical predictions, indicates that the band angle increases as the deviatoric stress state varies from axisymmetric compression to extension (decreasing N) The predictions lie within the variation of the data for axisymmetric extension ($\sqrt{3}N = -1$) and compression, ($\sqrt{3}N = 1$) but for the biaxial compression tests at intermediate values of N, the predicted angles are considerably below those observed. Possibly, this could reflect larger values of the sum $\mu + \beta$ than those for which the predictions are plotted (Figure 3). Recall, however, that if $\mu + \beta$ exceeds $\sqrt{3}$, α will exceed unity for some values of N and in these cases, the predicted angle will be $\theta = 90°$. Another possible reason for the predicted angles being smaller than observed is the development of anisotropy due to preferential microcrack growth in the axial direction. The calculations for axisymmetric compression that include anisotropy (Rudnicki (1977); see above) indicate that this would increase the fault angle.

Results for the two other rocks tested by Mogi (1967) were similar. For Westerly granite, the observed fault angles ranged from 68 to 71° for axisymmetric compression and from 78 to 83° for axisymmetric extension. For Solenhofen limestone, the values were from 58 to 64° for axisymmetric compression and from 66 to

72° for extension. For both axisymmetric compression and extension, the measured angles tend to decrease slightly with increasing mean stress. This trend is consistent with a decrease in $\mu + \beta$ with mean stress (see Figure 3), as found by Holcomb and Rudnicki (1998) for Tennessee marble.

Handin *et al.*(1967) tested Solenhofen limestone and Blair dolomite (and a brittle glass). Band angles for Solenhofen limestone in axisymmetric compression at room temperature and a strain rate of 10^{-4}/sec ranged from 58 to 74°. Values at higher temperatures (200 to 400°C) and a slower strain rate (10^{-7}/sec) ranged from 59 to 64°. For the Blair dolomite, the angles ranged from 53 to 72° at room temperature and a strain rate of 10^{-4}/sec and from 50 to 69° at higher temperatures and the lower strain rate.

Values for extension for both the dolomite and limestone were generally higher than for compression, consistent with the trend of the predictions. Many of the fractures (six of nine at room temperature and the higher strain rate for the limestone and all four for the dolomite) were, however, observed to occur perpendicular to the least compressive stress ($\theta = 90°$). Although the expression (Eqn. (11)) does predict $\theta = 90°$ in extension for sufficiently large $\beta + \mu$, fracture perpendicular to the least compressive stress suggests a failure mechanism of discrete fracture propagation rather than shear localization.

Handin *et al.*(1967) also conducted combined compression and torsion tests on solid and hollow cylinders. Because of the radial variation in stress in the solid cylinders, it is not possible to compare the results with the theory for homogeneous deformation outlined here. The tests on hollow cylinders achieved a range of N values but many of the fractures appear to be the result of discrete crack propagation (band angles perpendicular to least compressive stress). A plot of the results of the torsion tests against N exhibited considerable scatter and no consistent trend.

In contrast to the other rock types, the shear band angles for Castlegate sandstone are systematically smaller than predicted by the theory. Compactive deformation indicated by decreasing β with increasing confining pressure may explain some of the difference for this porous rock. Ongoing analysis of the data from the experiments suggests that the experimental determination of μ may also be a factor in the over-prediction of θ. The yield surface for Castlegate is characterized by a cap and therefore the local value of μ, when the stress path intersects the cap before overall shear yielding, may have a relatively large negative value. This would cause the predicted θ to be smaller. Further investigation of this issue is currently underway.

References

Chau, K.-T. and Rudnicki, J. W. Bifurcations of compressible pressure-sensitive materials in plane strain tension and compression, *J. Mech. Phys. Solids*, 1990, **38**, 875-898.

Handin, J., On the Coulomb-Mohr failure criterion, *J. Geophys. Res.*, 1969, **74**, 5343-5348.

Handin, J. Heard, J. C. and Magouirk, J. N., Effects of the intermediate principal stress on the failure of limestone, dolomite and glass at different temperatures and strain rates, *J. Geophys Res.*, 1967, **72**, 611-640.

Hill, R. and Hutchinson, J. W., Bifurcation phenomena in the plane tension test, *J. Mech. Phys. Solids*, 1975, **23**, 239-264.

Holcomb, D. and Rudnicki, J. W., Inelastic constitutive properties and shear localization in Tennessee marble, draft manuscript, 1998.

Jaeger, J. C. and Cook, N.G.W.,(1969) Fundamentals of Rock Mechanics, 2nd Edition, John Wiley and Sons, New York.

Mogi, K., Effect of intermediate principal stress on rock failure, *J. Geophys. Res.*, 1967, **72**, 5117-5131.

Mogi, K., Effect of the triaxial stress system on the failure of dolomite and limestone, Tectonophysics, 1971, **11**, 11-127.

Needleman, A., Non-normality and bifurcation in plane strain tension and compression, *J. Mech.Phys. Solids*, 1979, **27**, 231-254.

Perrin, G. and Leblond, J. B., Rudnicki and Rice's analysis of strain localization revisited, *J. Appl. Mech.*,1993, **60**, 842-846.

Rice, J. R., Rudnicki, J. W., A note on some features of the theory of localization of deformation, *Int. J. Solids Structures*,1980, **16**, 597-605.

Rudnicki, J. W., The effect of stress-induced anisotropy on a model of brittle rock failure as localization of deformation, in *Proc. 18th U.S. Sympos. Rock Mech. (1977)*, eds. F.-D. Wang and G. B. Clark, Johnson Pub. Co. pp. 3B4-1 —3B4-8.

Rudnicki, J. W. and Rice, J. R., Conditions for the localization of deformation in pressure-sensitive dilatant materials, *J. Mech. Phys. Solids*, 1975, **23**, 371-394, .

Young, N. J. B., Bifurcation phenomena in the plane compression test, *J. Mech.Phys. Solids*, 1976, **24**, 77-91.

Report Number (14) _SAND--98-0519C_
CONF-980620--

Publ. Date (11) _199802_
Sponsor Code (18) _DOE/ER , XF_
UC Category (19) _UC-400, DOE/ER_

DOE